PROCEEDINGS OF SCIENCE

Nucleon Energy-Energy Correlator in Lepton-Nucleon Collisions

Haotian Cao[a,b,*]

[a] *Department of Physics, Beijing Normal University, Beijing, 100875, China*

[b] *Key Laboratory of Multi-scale Spin Physics, Ministry of Education, Beijing Normal University, Beijing 100875, China*

E-mail: haotiancao@mail.bnu.edu.cn

The nucleon energy-energy correlator (NEEC) was proposed in [1] as a new way to study the nucleon structure. We present the factorization theorem that enables the measurement of the unpolarized NEEC in lepton-nucleon collisions. We present the complete spectrum for the observalbe. The corresponding collinear and transverse momentum-dependent logarithms are resummed to all orders with the accuracy of NLL and N^3LL, respectively. And the results in the full region are matched with $O(\alpha_s^2)$ fixed-order calculation.

25th International Spin Physics Symposium (SPIN 2023)
24-29 September 2023
Durham, NC, USA

*Speaker

PoS(SPIN2023)027

1. Introduction

Understanding nucleon structure and the formation of hadrons from partons is a key objective in particle physics. This pursuit remains at the forefront of exploration within the Standard Model, particularly at the forthcoming electron-ion collider (EIC) and future QCD facilities [2–4].

Conventional approach to the nucleon/nucleus tomography is to probe their transverse momentum dependent (TMD) structure functions through either the semi-inclusive deep inelastic scattering (SIDIS) [5–10] or the jet-based studies [11–24]. However, SIDIS requires knowledge of TMD fragmentation functions, while jets involve clustering procedures and high machine energy, both of which complicate the analysis.

Energy-Energy Correlation (EEC) is an event shape which stands out among other event shape observables for its simplicity and effectiveness in revealing the nucleon intrinsic transverse-dependent dynamics [25–27] and the scales of the quark-gluon plasma [28–31].

In Ref. [27], the EEC has been adapted to the deep inelastic scattering (DIS) process in the current fragmentation region (CFR), where the observed particles result from the fragmentation of the parton struck by the virtual photon and the outgoing parton fragments into the detected particles. It was shown that the EEC in this region can be used to extract the conventional TMDPDFs and the TMDFFs. On the other hand, in the target fragmentation region (TFR), where the outgoing particles propagate in the forward direction close to the incoming hadron beam, a variant of EEC, named nucleon energy-energy correlator (NEEC) was proposed in [1], which supplies a unique opportunity to reveal the intrinsic dynamics of nucleons. Notably, similar to EEC, NEEC manifests a remarkable phase transition between the perturbative parton and the non-perturbative free hadron phase [1]. NEEC has also been shown powerful in unraveling the on-set of gluon saturation [32] predicted by small-x physics. Furthermore, a joint measurement of NEEC in the TFR and CFR exhibits an exquisite signature of the linearly polarized gluons inside the nucleons [33]. The derivation of the NEEC factorization theorem and its NLL resummation were obtained in [34]. The complete spectrum for NEEC is presented in [35]

The definition of the NEEC observable is

$$\frac{d\Sigma_N}{dQ^2 d\theta} = \sum_i \int d\sigma(x_B, Q^2, p_i) x_B^{N-1} \frac{E_i}{E_P} \delta(\theta - \theta_i) \,. \tag{1}$$

Here $N > 1$ is a positive power, and $d\sigma$ is the differential cross section with Bjorken x_B and virtuality of the photon Q. p_i denotes the four-momentum of the particle detected by the calorimetry. The angle θ_i is the polar angle of p_i with respect to the nucleon beam. E_i and E_P are the energy of the detected particle and the incoming nucleon, respectively. The measurement is illustrated in Fig.1.

In the TFR and the TMD region, NEEC can be systematically analyzed using the factorized formula based on the soft-collinear effective theory (SCET) [36–41].

2. Factorization theorem

2.1 TMD region

In the TMD region, $\pi - \theta \ll 1$, the NEEC can be related to the single hadron production process $e + p \to e + a + X$ with a small transverse momentum of the observed hadron. The expression for

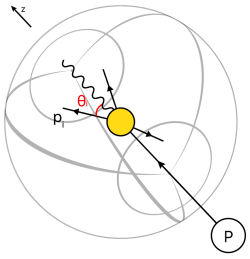

Figure 1: The EEC measurement in DIS. The sphere represents the detector that reports the energy and the angle of the final state particle.

$\Sigma_N(Q^2,\theta)$ is given by [27]:

$$\frac{d\Sigma_N}{dQ^2 d\theta} = \int dx_B x_B^{N-1} \sum_a \int d^2\mathbf{q}_T dz \frac{d\sigma_{e+p\to e+a+X}}{dQ^2 dx_B d^2 q_T dz} \frac{E_a}{E_p} \delta(\theta_{ap} - \theta)\,. \tag{2}$$

The factorization of the EEC can be obtained by approximating $\frac{E_a}{E_p}$ as $x_B z_a$:

$$\begin{aligned}\frac{d\Sigma_N}{dQ^2 d\theta} &= \int dx_B\, x_B^N H(Q^2,\mu) \int d^2 q_T \frac{d^2 b}{(2\pi)^2} \exp[-iq_T\cdot b] B_{f/p}(b, x_B, \mu, \nu) \\ &\times S(b,\mu,\nu) J_{f,\mathrm{EEC}}(b,\mu,\nu)\delta\left(\frac{2|q_T|}{Q} - \theta\right),\end{aligned} \tag{3}$$

where $B_{f/p}$ is the TMD beam function, S is the soft function and $b = |\mathbf{b}|$. $J_{f,\mathrm{EEC}}$ is the EEC (anti-)quark jet function defined as the first moments of the fragmentation functions $D_{a/f}$:

$$J_{f,\mathrm{EEC}} \equiv \sum_a \int_0^1 dz\, z D_{f/a}(z,b)\,. \tag{4}$$

2.2 Target Fragmentation Region

The expression for $\Sigma_N(Q^2,\theta)$ can be written as:

$$\frac{d\Sigma_N}{dQ^2 d\theta} = \frac{\alpha^2}{Q^4} \int dx_B x_B^{N-1} L_{\mu\nu} \int d^4x e^{iq\cdot x} \langle P|j^{\mu\dagger}(x)\,\hat{\mathcal{E}}(\theta)\, j^{\nu}(0)|P\rangle\,, \tag{5}$$

with $L_{\mu\nu}$ the lepton tensor the same as DIS. The inserted normalized asymptotic energy flow operator $\hat{\mathcal{E}}(\theta)$ measures the energy deposited in the detector at a given angle θ [42–45] normalized to the energy E_P of the incoming proton

$$\hat{\mathcal{E}}(\theta)|X\rangle \equiv \sum_{i\in X} \frac{E_i}{E_P}\delta(\theta - \theta_i)|X\rangle\,. \tag{6}$$

The contribution of the energy flow operator in the soft region will be power suppressed by the factor $\frac{E_i}{E_P}$.

We further match the hadron tensor in Eq. (5) to the SCET matrix as

$$\int d^4x e^{iq\cdot x}\,\langle P|j^{\dagger\mu}(x)\,\hat{\mathcal{E}}(\theta)\,j^{\nu}(0)|P\rangle \;=\; \int d^4x e^{iq\cdot x}\Big(C_q^{\mu\nu}(x)\langle P|\bar{\chi}_n(x^-)\frac{\gamma^+}{2}\hat{\mathcal{E}}(\theta)\chi_n(0)|P\rangle + C_g^{\mu\nu}(x)\langle P|\mathcal{B}_\perp(x^-)\hat{\mathcal{E}}(\theta)\mathcal{B}_\perp(0)|P\rangle\Big)\,, \tag{7}$$

which contains only the gauge invariant collinear quark and gluon fields χ and $\mathcal{B}_\perp$, respectively [46]. In addition, we have the soft Wilson lines Y and $\mathcal{Y}$ in the fundamental and the adjoint representation, respectively. Here we have used the fact that the soft Wilson lines decouple the interaction between the collinear and the soft sectors $[\hat{\mathcal{E}}, Y] = [\hat{\mathcal{E}}, \mathcal{Y}] = 0$, since $\hat{\mathcal{E}}(\theta)$ and $Y(\mathcal{Y})$ act on different sectors. We have also used the identity $Y^\dagger Y = \mathcal{Y}^\dagger\mathcal{Y} = 1$.

By recognizing that when the collinear operator $\hat{\mathcal{E}}(\theta)$ is replaced with the identity operator $1 = \sum_X |X\rangle\langle X|$, we recover the hadron tensor in the standard inclusive DIS cross section. Meanwhile, Eq. (5) reduce to the inclusive DIS cross section and the hard coefficients remain unaffected whether using the collinear operator $\hat{\mathcal{E}}(\theta)$ or the identity operator in the collinear function. We can establish that the hard tensors $C_q^{\mu\nu}$ and $C_g^{\mu\nu}$ are equivalent to the hard tensors in inclusive DIS.

Immediately, the factorization of the observable can be obtained:

$$\frac{d\Sigma_N}{dQ^2 d\theta} \;=\; \sum_{i=q,g}\int dx_B x_B^{N-1}\int\frac{dz}{z} f_\lambda \hat{\sigma}_{\lambda,i}\left(\frac{x_B}{z}, Q^2\right) f_{i,\mathrm{EEC}}(z, P^+\theta)\,. \tag{8}$$

where $f_{q,\mathrm{EEC}}$ is the quarks NEEC

$$f_{q,\mathrm{EEC}}(z,\theta) \equiv \int\frac{dy^-}{4\pi}e^{-izP^+\frac{y^-}{2}}\langle P|\bar{\chi}_n\left(\frac{y^-}{2}n^\mu\right)\frac{\gamma^+}{2}\hat{\mathcal{E}}(\theta)\chi_n(0)|P\rangle\,, \tag{9}$$

and $f_{g,\mathrm{EEC}}$ is the gluon NEEC

$$f_{g,\mathrm{EEC}}(z,\theta) = \int\frac{dy^-}{4\pi}e^{-izP^+\frac{y^-}{2}}P^+\langle P|\mathcal{B}_\perp\left(\frac{y^-}{2}n^\mu\right)\hat{\mathcal{E}}(\theta)\mathcal{B}_\perp(0)|P\rangle\,. \tag{10}$$

$\hat{\sigma}_{\lambda,i}$ is the partonic DIS cross section. The corresponding flux is given by $f_T = 1-y+\frac{y^2}{2}$, $f_L = 2-2y$.

We notice that in the TFR, the soft radiations are fully encompassed in the measurement, and therefore the soft modes do not lead to any logarithmic enhancement contributions. This is different from the TMD region measurement, where the soft contribution leads to the enhanced contribution which eventually gives rise to the perturbative Sudakov factor that suppresses the distribution in the TMD region exponentially.

When $\theta P^+ \gg \Lambda_{\mathrm{QCD}}$, the NEEC can be matched onto the collinear PDFs, with all θ dependence occurring only in the perturbative matching coefficients. In this way, since f_{EEC} is dimensionless, the $P^+\theta$ will show up in the form of $\ln\frac{P^+\theta}{\mu}$. Therefore, $\frac{d\Sigma_N}{dQ^2 d\theta}$ could also be written as

$$\frac{d\Sigma_N}{dQ^2 d\theta} \;=\; \frac{d\hat{\Sigma}_{T,N}}{dQ^2 d\theta} + 2\frac{d\hat{\Sigma}_{L,N}}{dQ^2 d\theta} + \frac{Q^4}{2s^2}\frac{d\hat{\Sigma}_{T,N-2}}{dQ^2 d\theta} - \frac{Q^2}{s}\left(\frac{d\hat{\Sigma}_{T,N-1}}{dQ^2 d\theta} + 2\frac{d\hat{\Sigma}_{L,N-1}}{dQ^2 d\theta}\right)\,, \tag{11}$$

where we defined

$$\frac{d\hat{\Sigma}_{\lambda,N}}{dQ^2 d\theta} \;=\; \sum_{i=q,g}\int du\, u^{N-1}\hat{\sigma}_{\lambda,i}\left(u, Q^2\right) f_{i,\mathrm{EEC}}\left(N, \ln\frac{Q\theta}{u\mu}\right)\,, \tag{12}$$

with $u = \frac{x_B}{z}$ and we have used the fact that $P^+ = \frac{Q}{x_B} = \frac{Q}{zu}$ in the Breit frame. The μ-dependence in other forms through the strong coupling and the collinear PDFs are suppressed in the $f_{i,\mathrm{EEC}}$, where $f_{i,\mathrm{EEC}}(N, \ln \frac{Q\theta}{u\mu})$ is the NEEC in the Mellin space,

$$f_{i,\mathrm{EEC}}(N, \ln \frac{Q\theta}{u\mu}) = \int_0^1 dz\, z^{N-1} f_{i,\mathrm{EEC}}(z, \ln \frac{Q\theta}{zu\mu})\,. \tag{13}$$

The NEEC satisfies the modified DGLAP evolution equation

$$\frac{d}{d\ln\mu^2} f_{i,\mathrm{EEC}}(N, \ln \frac{Q\theta}{u\mu}) = \sum_j \int d\xi \xi^{N-1} P_{ij}\,(\xi)\, f_{j,\mathrm{EEC}}(N, \ln \frac{Q\theta}{\xi\, u\mu})\,, \tag{14}$$

where P_{ij} is the vacuum splitting function. The solution of this RG equation at NLL level of accuracy is given in [34].

In the limit of extremely small angles, we anticipate the $d\Sigma_N/d\theta$ pattern indicates the presence of a free hadron phase where the energy is uniformly distributed. In this phase, the energy deposit within the region bounded by the polar angle being less than θ is proportional to θ^2. As NEEC is proportional to the distribution of energy with respect to the polar angle, We expect

$$\frac{d\Sigma_N}{d\theta}|_{\mathrm{NP}} \propto \theta\,. \tag{15}$$

The analogous pattern has also been observed in the final state jet through the utilization of CMS open data [47].

3. Numerical Results

In this section, we explore the NEEC distributions with two distinct collision energies. The interaction of 18 GeV electrons with 275 GeV protons at the EIC with $\sqrt{s} = 140.7$ GeV, and the interaction of 22 GeV electrons with 2 GeV protons at CEBAF with $\sqrt{s} = 13.3$ GeV.

For the EIC kinematics, we set the parameters as $N = 4$ and $Q = 20$ GeV, while for the CEBAF kinematics, we consider $N = 4$ and $Q = 3$ GeV. For all the numerical results, we use the `PDF4LHC15_nnlo_mc` PDF sets [48] with the associated strong coupling provided by `LHAPDF6` [49].

We validate the factorization formalism by comparing the leading singular $\ln\theta$ contributions predicted by the factorization theorem with the complete α_s and α_s^2 calculations of the distribution $d\Sigma_N/dy$, where $y \equiv \ln\tan\frac{\theta}{2}$. The comparison is shown in Fig. 2 utilizing EIC kinematics. The full fixed-order calculations are obtained numerically using `nlojet++` [50]. Remarkably, in both the small y and large y regions, we observe excellent agreement between the leading singular terms predicted by the factorization formula and the full fixed-order calculations.

In the TMD region and the TFR, the logarithmic enhancements can spoil the convergence of the perturbative expansion. Therefore, the resummation of these logarithms to all orders in the strong coupling is necessary for reliable predictions to compare with experimental data.

The final distributions without non-perturbative effects for EIC and CEBAF are presented in the left and right panels of Fig. 3, respectively. In the TMD region, we match the $\mathrm{N^2LL}$ ($\mathrm{N^3LL}$) resummed distributions to the QCD LO (NLO) ones. In the TFR, we match the NLL resummed

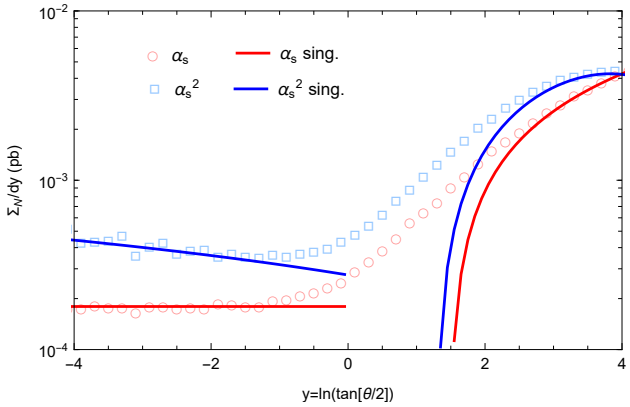

Figure 2: Comparison between the $\ln\theta$ leading singular contributions with the full fixed-order calculations in both the forward and backward regions.

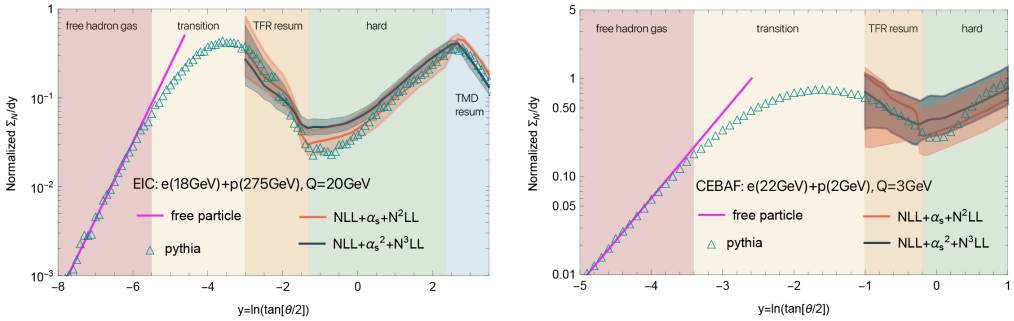

Figure 3: Comparison of EEC between the SCET predictions without non-perturbative effects, free hadron gas model, and PYTHIA simulations running without hadronization modeling. The left panel displays the results for EIC kinematics, while the right panel showcases the results for CEBAF kinematics.

distributions to the QCD LO (NLO) ones. We compare our calculations to `PYTHIA` [51, 52] simulations without a hadronization modeling.

In the perturbative region, the matching result agrees reasonably well with the partonic `PYTHIA` simulation. In the extreme forward region, when $y < -5.5$ in EIC kinematics and $y < -3.4$ in CEBAF kinematics, we fit the un-normalized `PYTHIA` distribution with the non-perturbative model $a_{\rm NP}\theta$ to observe the free hadron gas phase. Even without hadronization, We observe a nearly perfect $d\Sigma_N/dy \propto \theta^2$ scaling, as expected above in Eq. (15), corresponding to uniformly distributed partons.

Furthermore, in Fig. 3, we observe a distinct phase transition. The transition from the TFR resummation region to the free hadron gas region, connected by a non-perturbative transition region. When comparing the EIC kinematics distribution to the CEBAF kinematics distribution, we observe that the free hadron gas region and the transition region shift to larger angles in the CEBAF kinematics distribution. This shift is expected since the transition occurs as $\theta \sim O(\Lambda_{\rm QCD}/Q)$. Consequently, CLAS holds the potential for probing NEEC in the non-perturbative region, which essentially enables direct imaging of the confining transition to free hadrons.

In Fig.4, we compare the simulated `PYTHIA` result with and without hadronization for both EIC and CEBAF kinematics. We observe that for $y < -5.5$ in EIC kinematics and $y < -3.4$ in CEBAF

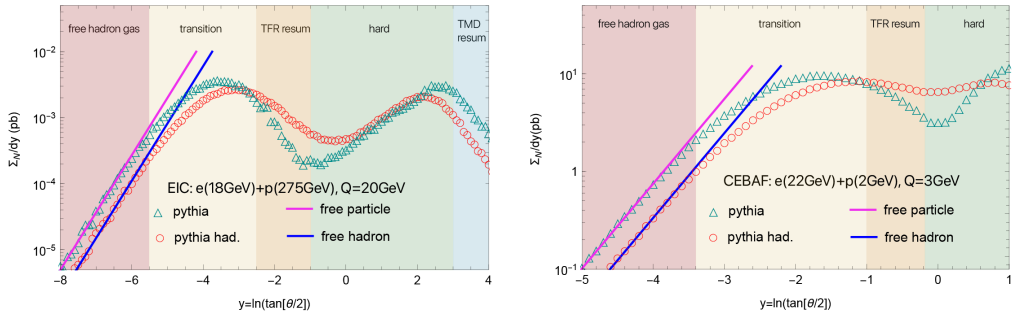

Figure 4: Comparison of EEC between PYTHIA simulations with and without hadronization. The left panel displays the results for EIC kinematics, while the right panel showcases the results for CEBAF kinematics.

kinematics, the $d\Sigma_N/dy \propto \theta^2$ scaling persists, indicating the presence of uniformly distributed hadrons.

4. Conclusion

In this work, we review the factorization theorem for the NEEC measurement in lepton-nucleon collisions. The singular distributions can be derived from the factorized formula, which are compared against the full fixed-order QCD calculations up to NLO. In the extremely small angle limit, the free hadron gas model is introduced to investigate the non-perturbative distribution. We compared our predictions to partonic PYTHIA simulations. Between the hadron gas phase region and the perturbative resummation region, a transition phase is observed. We note that the transition region from perturbative parton phase to non-perturbative region for CEBAF begins at $\theta \sim 0.7$ rad, indicating CLAS may have a good opportunity to probe the non-perturbative NEEC.

Acknowledgments

H. C. is supported by the Natural Science Foundation of China under contract No. 12175016.

References

[1] X. Liu and H.X. Zhu, *Nucleon Energy Correlators*, *Phys. Rev. Lett.* **130** (2023) 091901 [2209.02080].

[2] R. Abdul Khalek et al., *Science Requirements and Detector Concepts for the Electron-Ion Collider: EIC Yellow Report*, 2103.05419.

[3] E.D.P.A. Panel, *Report from the EIC Detector Proposal Advisory Panel*, .

[4] A. Accardi et al., *Strong Interaction Physics at the Luminosity Frontier with 22 GeV Electrons at Jefferson Lab*, 2306.09360.

[5] J.C. Collins, A.V. Efremov, K. Goeke, S. Menzel, A. Metz and P. Schweitzer, *Sivers effect in semi-inclusive deeply inelastic scattering*, *Phys. Rev. D* **73** (2006) 014021 [hep-ph/0509076].

[6] W. Vogelsang and F. Yuan, *Single-transverse spin asymmetries: From DIS to hadronic collisions*, *Phys. Rev. D* **72** (2005) 054028 [hep-ph/0507266].

[7] HERMES collaboration, *Observation of the Naive-T-odd Sivers Effect in Deep-Inelastic Scattering*, *Phys. Rev. Lett.* **103** (2009) 152002 [0906.3918].

[8] A. Bacchetta and M. Radici, *Constraining quark angular momentum through semi-inclusive measurements*, *Phys. Rev. Lett.* **107** (2011) 212001 [1107.5755].

[9] M.G. Echevarria, A. Idilbi, Z.-B. Kang and I. Vitev, *QCD Evolution of the Sivers Asymmetry*, *Phys. Rev. D* **89** (2014) 074013 [1401.5078].

[10] I. Scimemi and A. Vladimirov, *Non-perturbative structure of semi-inclusive deep-inelastic and Drell-Yan scattering at small transverse momentum*, *JHEP* **06** (2020) 137 [1912.06532].

[11] Z.-B. Kang, J. Terry, A. Vossen, Q. Xu and J. Zhang, *Transverse Lambda production at the future Electron-Ion Collider*, *Phys. Rev. D* **105** (2022) 094033 [2108.05383].

[12] X. Liu and H. Xing, *The Time-reversal Odd Side of a Jet*, 2104.03328.

[13] Z.-B. Kang, K. Lee, D.Y. Shao and F. Zhao, *Spin asymmetries in electron-jet production at the future electron ion collider*, *JHEP* **11** (2021) 005 [2106.15624].

[14] H.T. Li, Z.L. Liu and I. Vitev, *Heavy flavor jet production and substructure in electron-nucleus collisions*, *Phys. Lett. B* **827** (2022) 137007 [2108.07809].

[15] W.K. Lai, X. Liu, M. Wang and H. Xing, *Unveiling Nucleon 3D Chiral-Odd Structure with Jet Axes*, 2205.04570.

[16] Z.-B. Kang, K. Lee, D.Y. Shao and F. Zhao, *Spin Asymmetries in Electron-jet Production at the EIC*, 2201.04582.

[17] M. Arratia, Z.-B. Kang, S.J. Paul, A. Prokudin, F. Ringer and F. Zhao, *Neutrino-tagged jets at the Electron-Ion Collider*, 2212.02432.

[18] H.-y. Liu, K. Xie, Z. Kang and X. Liu, *Single inclusive jet production in pA collisions at NLO in the small-x regime*, *JHEP* **07** (2022) 041 [2204.03026].

[19] P. Caucal, F. Salazar, B. Schenke and R. Venugopalan, *Back-to-back inclusive dijets in DIS at small x: Sudakov suppression and gluon saturation at NLO*, *JHEP* **11** (2022) 169 [2208.13872].

[20] L. Wang, L. Chen, Z. Gao, Y. Shi, S.-Y. Wei and B.-W. Xiao, *Forward inclusive jet productions in pA collisions*, *Phys. Rev. D* **107** (2023) 016016 [2211.08322].

[21] I. Ganguli, A. van Hameren, P. Kotko and K. Kutak, *Forward γ+jet production in proton-proton and proton-lead collisions at LHC within the FoCal calorimeter acceptance*, *Eur. Phys. J. C* **83** (2023) 868 [2306.04706].

[22] P. Caucal, F. Salazar, B. Schenke, T. Stebel and R. Venugopalan, *Back-to-back inclusive dijets in DIS at small x: gluon Weizsäcker-Williams distribution at NLO*, *JHEP* **08** (2023) 062 [2304.03304].

[23] A. van Hameren, H. Kakkad, P. Kotko, K. Kutak and S. Sapeta, *Searching for saturation in forward dijet production at the LHC*, *Eur. Phys. J. C* **83** (2023) 947 [2306.17513].

[24] P. Caucal, F. Salazar, B. Schenke, T. Stebel and R. Venugopalan, *Back-to-back inclusive dijets in DIS at small x: Complete NLO results and predictions*, 2308.00022.

[25] H.T. Li, I. Vitev and Y.J. Zhu, *Transverse-Energy-Energy Correlations in Deep Inelastic Scattering*, *JHEP* **11** (2020) 051 [2006.02437].

[26] A. Ali, G. Li, W. Wang and Z.-P. Xing, *Transverse energy–energy correlations of jets in the electron–proton deep inelastic scattering at HERA*, *Eur. Phys. J. C* **80** (2020) 1096 [2008.00271].

[27] H.T. Li, Y. Makris and I. Vitev, *Energy-energy correlators in Deep Inelastic Scattering*, *Phys. Rev. D* **103** (2021) 094005 [2102.05669].

[28] Z. Yang, Y. He, I. Moult and X.-N. Wang, *Probing the Short-Distance Structure of the Quark-Gluon Plasma with Energy Correlators*, 2310.01500.

[29] C. Andres, F. Dominguez, R. Kunnawalkam Elayavalli, J. Holguin, C. Marquet and I. Moult, *Resolving the Scales of the Quark-Gluon Plasma with Energy Correlators*, 2209.11236.

[30] C. Andres, F. Dominguez, J. Holguin, C. Marquet and I. Moult, *A coherent view of the quark-gluon plasma from energy correlators*, *JHEP* **09** (2023) 088 [2303.03413].

[31] C. Andres, F. Dominguez, J. Holguin, C. Marquet and I. Moult, *Seeing Beauty in the Quark-Gluon Plasma with Energy Correlators*, 2307.15110.

[32] H.-Y. Liu, X. Liu, J.-C. Pan, F. Yuan and H.X. Zhu, *Nucleon Energy Correlators for the Color Glass Condensate*, 2301.01788.

[33] X.L. Li, X. Liu, F. Yuan and H.X. Zhu, *Illuminating Nucleon Gluon Interference via Calorimetric Asymmetry*, 2308.10942.

[34] H. Cao, X. Liu and H.X. Zhu, *Toward precision measurements of nucleon energy correlators in lepton-nucleon collisions*, *Phys. Rev. D* **107** (2023) 114008 [2303.01530].

[35] H. Cao, H.T. Li and Z. Mi, *Bjorken x weighted Energy-Energy Correlators from the Target Fragmentation Region to the Current Fragmentation Region*, 2312.07655.

[36] C.W. Bauer, S. Fleming and M.E. Luke, *Summing Sudakov logarithms in B —gt; X(s gamma) in effective field theory*, *Phys.Rev.* **D63** (2000) 014006 [hep-ph/0005275].

[37] C.W. Bauer, S. Fleming, D. Pirjol and I.W. Stewart, *An Effective field theory for collinear and soft gluons: Heavy to light decays*, *Phys.Rev.* **D63** (2001) 114020 [hep-ph/0011336].

[38] C.W. Bauer and I.W. Stewart, *Invariant operators in collinear effective theory*, *Phys.Lett.* **B516** (2001) 134 [hep-ph/0107001].

[39] C.W. Bauer, D. Pirjol and I.W. Stewart, *Soft collinear factorization in effective field theory*, *Phys.Rev.* **D65** (2002) 054022 [hep-ph/0109045].

[40] C.W. Bauer, S. Fleming, D. Pirjol, I.Z. Rothstein and I.W. Stewart, *Hard scattering factorization from effective field theory*, *Phys.Rev.* **D66** (2002) 014017 [hep-ph/0202088].

[41] M. Beneke, A. Chapovsky, M. Diehl and T. Feldmann, *Soft collinear effective theory and heavy to light currents beyond leading power*, *Nucl.Phys.* **B643** (2002) 431 [hep-ph/0206152].

[42] N.A. Sveshnikov and F.V. Tkachov, *Jets and quantum field theory*, *Phys. Lett. B* **382** (1996) 403 [hep-ph/9512370].

[43] F.V. Tkachov, *Measuring multi - jet structure of hadronic energy flow or What is a jet?*, *Int. J. Mod. Phys. A* **12** (1997) 5411 [hep-ph/9601308].

[44] G.P. Korchemsky and G.F. Sterman, *Power corrections to event shapes and factorization*, *Nucl. Phys. B* **555** (1999) 335 [hep-ph/9902341].

[45] C.W. Bauer, S.P. Fleming, C. Lee and G.F. Sterman, *Factorization of e+e- Event Shape Distributions with Hadronic Final States in Soft Collinear Effective Theory*, *Phys. Rev. D* **78** (2008) 034027 [0801.4569].

[46] I.W. Stewart, F.J. Tackmann and W.J. Waalewijn, *The Quark Beam Function at NNLL*, *JHEP* **09** (2010) 005 [1002.2213].

[47] P.T. Komiske, I. Moult, J. Thaler and H.X. Zhu, *Analyzing N-Point Energy Correlators inside Jets with CMS Open Data*, *Phys. Rev. Lett.* **130** (2023) 051901 [2201.07800].

[48] J. Butterworth et al., *PDF4LHC recommendations for LHC Run II*, *J. Phys. G* **43** (2016) 023001 [1510.03865].

[49] A. Buckley, J. Ferrando, S. Lloyd, K. Nordström, B. Page, M. Rüfenacht et al., *LHAPDF6: parton density access in the LHC precision era*, *Eur. Phys. J. C* **75** (2015) 132 [1412.7420].

[50] Z. Nagy and Z. Trocsanyi, *Three-jet event-shapes in lepton-proton scattering at next-to-leading order accuracy*, *Phys. Lett. B* **634** (2006) 498 [hep-ph/0511328].

[51] T. Sjöstrand, S. Ask, J.R. Christiansen, R. Corke, N. Desai, P. Ilten et al., *An introduction to PYTHIA 8.2*, *Comput. Phys. Commun.* **191** (2015) 159 [1410.3012].

[52] C. Bierlich et al., *A comprehensive guide to the physics and usage of PYTHIA 8.3*, 2203.11601.